THE JOURNAL OF PHYSICAL CHEMISTRY B
A JOURNAL OF THE AMERICAN CHEMICAL SOCIETY

pubs.acs.org/JPCB

Article

Excited State Rotational Freedom Impacts Viscosity Sensitivity in Arylcyanoamide Fluorescent Molecular Rotor Dyes

Rachel S. Ehrlich, Saswata Dasgupta, R. Erin Jessup, Kristine L. Teppang, Alexander L. Shiao, Kun Yong Jeoung, Xuanmin Su, Aashish Shivkumar, Emmanuel A. Theodorakis, Francesco Paesani, and Jerry Yang*

Cite This: *J. Phys. Chem. B* 2024, 128, 3946–3952

Read Online

ACCESS | Metrics & More | Article Recommendations | Supporting Information

ABSTRACT: The microviscosity of intracellular environments plays an important role in monitoring cellular function. Thus, the capability of detecting changes in viscosity can be utilized for the detection of different disease states. Viscosity-sensitive fluorescent molecular rotors are potentially excellent probes for these applications; however, the predictable relationships between chemical structural features and viscosity sensitivity are poorly understood. Here, we investigate a set of arylcyanoamide-based fluorescent probes and the effect of small aliphatic substituents on their viscosity sensitivity. We found that the location of the substituents and the type of π-network of the fluorophore can significantly affect the viscosity sensitivity of these fluorophores. Computational analysis supported the notion that the excited state rotational energy barrier plays a dominant role in the relative viscosity sensitivity of these fluorophores. These findings provide valuable insight into the design of molecular rotor-based fluorophores for viscosity measurement.

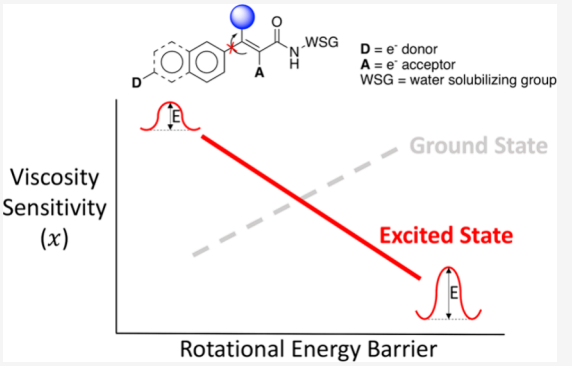

INTRODUCTION

Variations in the microviscosity of cellular organelles and biomolecules are an important metric for measuring cellular function.[1] For instance, changes in membrane viscosity are associated with a number of diseases such as diabetes, cardiovascular disease, and Alzheimer's Disease.[2−5] To better measure and monitor such changes, researchers often utilize molecular rotor-based fluorophores to study these systems.[6,7] Fluorescent molecular rotors (FMRs) are a class of fluorescent probes with an electron-rich donor (D) in conjugation through a π-scaffold to an electron-poor acceptor (A), separated by rotatable single bonds.[8−10] When achieving a locally excited (LE) state after photoexcitation, molecular rotors release energy either through fluorescence emission or by entering a twisted intramolecular charge transfer (TICT) state that can relax to the ground state through nonradiative decay mechanisms.[10] The microviscosity of the surrounding environment can affect the rate of internal molecular rotation as the frequency of rotation decreases with increasing local viscosity of the surrounding milieu.[11,12] Here, the internal rotation of the FMR is less hindered in low viscosity environments, and molecules can more easily adopt a TICT state, leading to nonradiative relaxation and lower fluorescence intensity.[13] As the viscosity of the environment increases, the resistance to rotation also increases, leading to a higher energy barrier to form the TICT state.[14] This effect of high viscosity environments results in a lower rate of nonradiative relaxation and a higher probability of radiative relaxation, leading to increased fluorescence intensity.

There have been several examples of fluorophores used as viscosity sensors, including classical probes such as DCVJ and CCVJ, BODIPYs, and Thioflavin T (ThT) analogues.[2,15] Many groups have reported attempts to tailor microenvironment sensitivity of these viscosity sensors through structure−activity relationship studies of synthetic analogue libraries.[2,6,13] For instance, a recent report on a family of BODIPY-based dyes showed that the introduction of methyl groups to the phenyl ring of BODIPY could inhibit the free rotation of the phenyl ring, leading to a decrease in the viscosity sensitivity and an increase in quantum yield compared to the unsubstituted BODIPY core.[16]

Previously, we reported a fluorescent molecular rotor aryl cyano amide (ARCAM **1**; Figure 1) that binds with high specificity to misfolded protein aggregates known as amyloids, which are the pathological hallmark of many neurodegenerative diseases.[17−19] This probe shares a common feature of molecular rotor amyloid-binding probes, where it exhibits a

Received: January 3, 2024
Revised: March 12, 2024
Accepted: March 28, 2024
Published: April 16, 2024

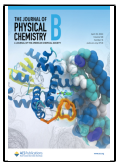

https://doi.org/10.1021/acs.jpcb.4c00033
J. Phys. Chem. B 2024, 128, 3946−3952

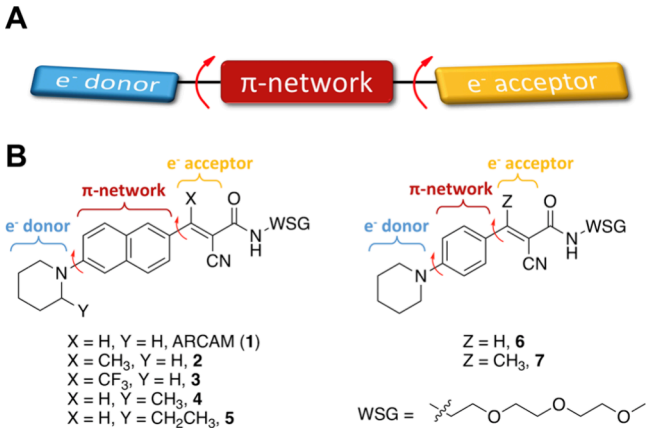

Figure 1. (A) Generalized structure for fluorescent molecular rotor probes. (B) Probes examined for viscosity sensitivity with different structural features highlighted.

large fluorescence enhancement upon binding to the hydrophobic pocket of an amyloid. This fluorescence increase is putatively due to the difference in free rotation about its single bonds when in solution compared to when bound to the sterically restricting binding pocket of an amyloid.

We also developed a series of ARCAM analogues with small, aliphatic substituents near the two rotatable single bonds that we thought most affected the planarity of the molecule (Figure 1, probes **2**−**5**) and investigated how these substituents affected their fluorescence enhancement and binding affinity to aggregated forms of amyloid-β (Aβ) peptides, the major component of senile plaques in Alzheimer's Disease.[20] We observed that introducing substituents in the vinylic position of **1** (as in **2** and **3**) lowered the overall fluorescence intensity of the free probes in solution but increased their fluorescence enhancement upon binding to Aβ compared to probe **1**. On the other hand, substituents in the 2-piperidinyl position of **1** (as in **4** and **5**) did not greatly affect the fluorescence intensity of the free probe and only lowered the amyloid-bound fluorescence intensity compared to probe **1**. These changes in fluorescence intensity were unrelated to differences in their binding affinity for aggregated Aβ and appeared to be attributed to the intrinsic properties of the probes.

Here, we now examined these compounds, as well as two new ARCAM analogues (probes **6** and **7**), for their sensitivity to changes in microviscosity, to gain additional insight on the effect of small aliphatic substitutions on the ARCAM scaffold on their emissive properties. We observed that only the vinylic substituents and not the 2-piperidinyl substituents affect the viscosity sensitivity of these probes and that an increase or decrease in viscosity sensitivity depended on the type of π-scaffold within the probe. This investigation showed that introducing small aliphatic substituents at the periphery of the π-network can be used to modify the viscosity sensitivity of fluorescent probes. Computational studies suggest that it is the excited state rotational energy barrier that most strongly affects the viscosity sensitivity of these FMRs.

EXPERIMENTAL METHODS

Chemicals and Methods. All reagents were purchased from commercial sources and used without further purification, except where noted. Air- and moisture-sensitive liquids and solutions were transferred via syringe. Organic solutions were concentrated by rotary evaporation below 45 °C at approximately 20 mmHg. All nonaqueous reactions were carried out under anhydrous conditions. Reactions were monitored by thin-layer chromatography (TLC) carried out on 0.25 mm Dynamic Adsorbents, Inc. silica gel plates (60F-254) and visualized under UV light and/or developed by dipping in solutions of 0.75% potassium permanganate ($KMnO_4$) and applying heat. Dynamic Adsorbents, Inc. silica gel (60, particle size of 0.040−0.063 mm) was used for flash chromatography. Deuterated solvents were purchased from Cambridge Isotope Laboratories, Inc. ^{1}H and ^{13}C NMR spectra were obtained on either a Varian 400/500 MHz or Bruker 300 MHz spectrometer and calibrated using the residual nondeuterated solvent as an internal reference. The following abbreviations were used to explain the multiplicities: s = singlet, d = doublet, t = triplet, q = quartet, m = multiplet, br = broad. Low-resolution MS analysis was performed on a Micromass Quattro Ultima triple quadrupole mass spectrometer with an electrospray ionization (ESI) source. High-resolution MS analysis was performed using Agilent 6230 Accurate-Mass TOFMS with an electrospray ionization (ESI) source by the Molecular Mass Spectrometry Facility (MMSF) in the Department of Chemistry and Biochemistry at the University of California, San Diego. Fluorescence characterization was performed using a Molecular Devices SpectraMax i3x Multi-Mode Microplate Reader. HPLC characterization of all final probes was conducted using an Agilent 1260 Infinity II Quaternary Pump System, where 10 μL of the probe at a final concentration of 200 μM (in 2.5% DMSO/H_2O) was injected into a 150 mm × 3 mm, 2.7 μm particle size C18 column (Agilent InfinityLab Poroshell 120-693975-302T). Elution conditions (Solvent A: H_2O (0.1% trifluoroacetic acid, TFA), Solvent B: acetonitrile): 0−2 min 5% B, 2−20 min 5−95% B, 20−22 min 95% B, 22−24 min 95−0% B, 24−30 min 0% B at 1 mL/min.

Quantum Yield Measurements. Quantum yields for probes **1**−**5** were reported previously.[20] The following method was used for determining the quantum yields for probes **6** and **7**. Briefly, the absorbance spectrum of each probe (in 5% DMSO/H_2O) was measured, in addition to the absorbance spectrum for the reference standard (coumarin 30, Φ = 0.67 in acetonitrile for probe **6**, quinine sulfate, Φ = 0.54 in 0.1 M H_2SO_4 for probe **7**).[21,22] The wavelength at which the two normalized absorbance curves intersected was used as the excitation wavelength. A dilution of each probe and the standard was made with absorbance values at the excitation wavelength in the range of 0−0.1 absorbance units. At each concentration, the emission spectra for each probe and the standard were measured. Technical triplicates of these experiments were performed for all probes, and the averages were recorded. From these emission spectra, the area under the curve was calculated and plotted against the absorbance at each concentration (see Figures S1 and S2). The data were fitted to eq 1 to obtain estimates for Φ:

$$\Phi_p = \Phi_r \left(\frac{A_r}{A_p}\right)\left(\frac{E_p}{E_r}\right)\left(\frac{\eta_p}{\eta_r}\right)^2 \quad (1)$$

where Φ represents the quantum yield, A represents the absorbance, E represents the integrated fluorescence emission, η represents the refractive index of the solvent,[23−25] and the "p" and "r" subscripts signify the probe or the reference compound, respectively.

https://doi.org/10.1021/acs.jpcb.4c00033
J. Phys. Chem. B 2024, 128, 3946−3952

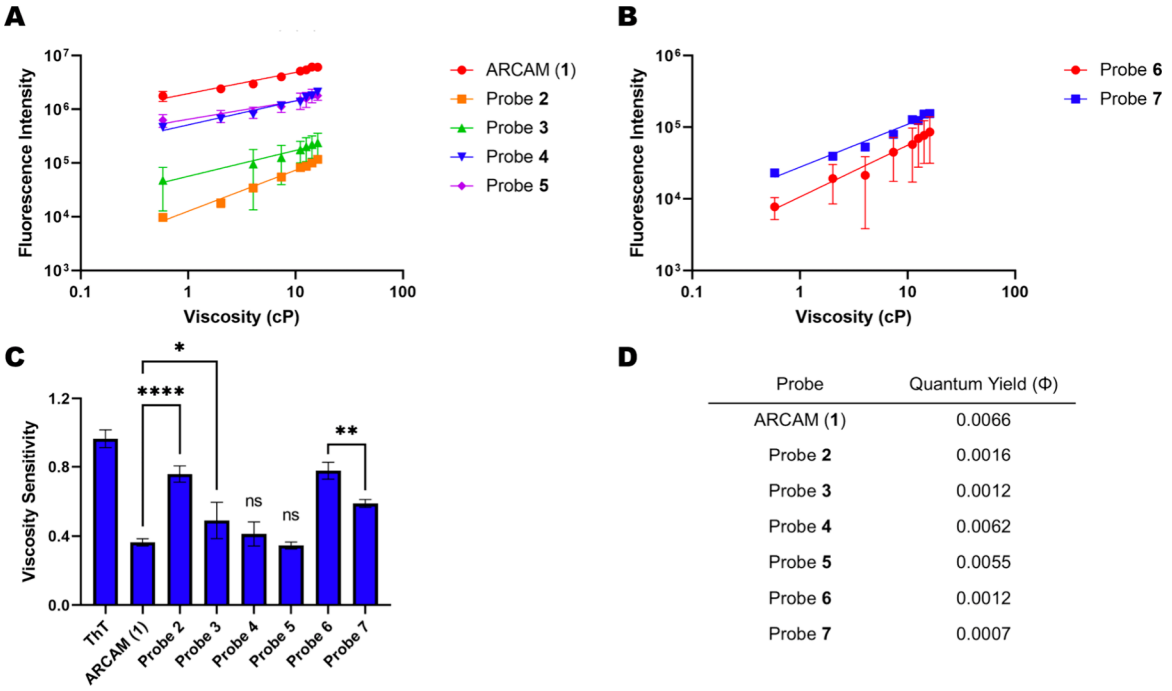

Figure 2. Viscosity sensitivity data. (A) Log−log plot of fluorescence intensity vs viscosity for ARCAM (**1**) and probes **2**−**5**. (B) Log−log plot of fluorescence intensity vs viscosity for probes **6** and **7**. (C) Viscosity sensitivity data for ThT and probes **1**−**7**. Asterisks indicate statistically significant differences by one-way ANOVA between probes (****p < 0.0001 ***p < 0.001, **p < 0.01, *p < 0.05, ns = not significant). (D) Measured quantum yields of probes **1**−**7** in water (with 5% DMSO to aid with solubility).

Viscosity Sensitivity Measurements. All samples used were prepared from a DMSO stock solution and hence contained 5 v/v% DMSO, which was assumed to have a negligible effect on the viscosity of the total solution.[26] The viscosity of each solution mixture was calculated using eq 2:

$$\ln \eta_{\text{mix}} = \sum_{i=1}^{2} w_i \cdot \ln \eta_i \tag{2}$$

where η_{mix} and η_i are the viscosities of the mixture and individual components, respectively, and w_i is the weight fraction of each component i. The weight fraction was calculated by using eq 3:

$$w_i = \frac{\phi_i \rho_i}{(\phi\rho)_{\text{total}}} \tag{3}$$

where ϕ is the volume fraction and ρ is the density.

Each probe was dissolved in one of the mixtures of solutions found in Table S1. These ratios of methanol-ethylene glycol were chosen to give an even distribution of data points over the entire viscosity window used.[26]

Probes **1**−**6** were dissolved in each solution at a concentration of 4 μM, while probe **7** was dissolved at a concentration of 50 μM to account for the difference in brightness. For each sample, the fluorescence emission at the maximum wavelength was measured and plotted in a log−log plot against the viscosity. The data were fit to a power trendline (see eq 5), and the viscosity sensitivity (x) was obtained from the exponent of the trendline equation.

Computational Analysis. DFT calculations were performed using Q-Chem 5.6.[27] Geometry optimizations in the ground state (S_0) and excited state (S_1) were performed in the gas phase. All the geometry optimizations and energy calculations employ the ωB97X-D functional,[28] in combination with the def2-TZVPP basis set and SG-3 integration grid[29] for both ground and excited states. Data from θ = −180 to 180° and from ϕ = 0 to −180° were calculated for all probes.

RESULTS AND DISCUSSION

Design and Synthesis of Probes to Study the Effect of Restricted Rotation on Viscosity Sensitivity in ARCAM-Based Fluorophores. A previous report with BODIPY dyes[16] showed that the introduction of methyl groups near the rotatable single bonds of a molecular rotor was sufficient to affect rotational freedom and viscosity sensitivity. We, therefore, hypothesized that the small aliphatic substituents near the rotatable single bonds in ARCAM (**1**) could also affect rotational freedom and viscosity sensitivity in ARCAM analogues (**2**−**5**) compared to **1**. To determine whether the π-scaffold could also play a role in the viscosity sensitivity of these probes, we designed and synthesized two additional fluorescent compounds in which the naphthyl π-scaffold in **1** was replaced with a benzyl group and evaluated the relative viscosity sensitivity of probes that did (**7**) or did not (**6**) carry a methyl group on the vinylic position. The synthesis of probes **6** and **7** is described in the Supporting Information.

Viscosity Sensitivity Measurements. To determine the effect of environmental viscosity on the observed fluorescence intensity of each probe, the fluorescence intensity was measured in mixtures of methanol and ethylene glycol (Table S1 and Figure S3). Solvents of similar polarity were used so that any solvatochromic properties of the fluorophores would be negligible.[15] Typically, in highly viscous environments, excited state relaxation occurs through fluorescence emission in a larger proportion than in low viscosity environments. This trend leads to a relationship where the fluorescence intensity is proportional to the solvent viscosity. Förster and Hoffmann found a nonlinear relationship between

https://doi.org/10.1021/acs.jpcb.4c00033
J. Phys. Chem. B 2024, 128, 3946−3952

fluorescent quantum yield (Φ) and viscosity (η) shown in eq 4[30]:

$$\log \Phi = x \log \eta + C \quad (4)$$

where x is defined as the viscosity sensitivity and C is an empirical proportionality constant. Rather than calculating the quantum yield at each individual viscosity, it is often more practical to calculate x in terms of the directly measurable parameter of fluorescence intensity (I) as it is linearly proportional to quantum yield.[31] In this case, eq 4 can be rewritten as eq 5[10]:

$$I = \alpha \eta^{x} \quad (5)$$

where α is a new constant defined as 10^{C}. The viscosity sensitivity, x, gives information about how strongly changes in environmental viscosity affect the fluorescence intensity of a specific fluorophore.

We first used Thioflavin T (ThT) as a positive control in this assay and obtained a viscosity sensitivity value for ThT that was consistent with literature values.[13] For the ARCAM analogues, we expected the four rotationally restricted analogues (**2**–**5**) to exhibit a lower viscosity sensitivity compared to ARCAM (**1**) since substitution in proximity to the rotatable single bonds should lead to a higher barrier to rotation. Interestingly, this prediction was not what we observed (Figure 2A,C). Probes **2** and **3** exhibited a significantly higher viscosity sensitivity than ARCAM, while probes **4** and **5** had no significant difference in viscosity sensitivity compared to ARCAM. With regard to probes **4** and **5**, the similarities they exhibited in viscosity sensitivity compared to ARCAM (**1**) suggest that the rotatability of the naphthalene-piperidine bond is not greatly affected by the introduction of a methyl or ethyl group on the 2-position of the piperidine ring.

The most surprising result compared to our original hypothesis was the significant increase in viscosity sensitivity exhibited by probes **2** and **3** compared to ARCAM (**1**). To determine if the increase in viscosity sensitivity by introducing substituents on this vinylic position was specific to this scaffold, we compared the relative viscosity sensitivity of probes **6** and **7**, which are direct analogues of probes **1** and **2**, respectively, with a benzyl π-network instead of a naphthyl π-network. Compared to ARCAM (**1**), probe **6** had a higher viscosity sensitivity; however, introducing the vinylic methyl substituent in probe **7** decreased the viscosity sensitivity compared to that of **6** (Figure 2B,C). Contrary to the probes with the naphthyl scaffold, this observation appears to be more consistent with our initial hypothesis that the vinylic methyl substituent would restrict the rotational freedom of probe **7** compared to probe **6**. Quantum yields were also calculated for all probes, and we found that introducing small aliphatic groups on the vinylic position in **2**, **3**, and **7** lowered the quantum yields (Figure 2D and Figure S2) compared to the parent compounds **1** and **6** (Figure 2D and Figure S1). On the other hand, probes **4** and **5** had similar quantum yields with parent probe **1**, supporting the notion that substitution distant from the conjugating motif does not substantially affect the emissive properties of the probe.

Computational Analysis. The viscosity sensitivity measurements showed that the effect of the addition of small aliphatic substituents added to the vinylic position of probes **1** and **6** was not consistent with simple predictions based on literature precedence[16] and also depended on the nature of the π-network separating the electron donor and acceptor in the molecular rotor. We, therefore, turned to computational analysis to gain additional insight on the effect of these vinylic substitutions on rotational freedom as rotational freedom is an essential parameter that governs viscosity sensitivity of molecular rotors.[13] We focused these computational studies on comparing the rotational energy barriers of probes **1** versus **2** as well as probes **6** versus **7** as these pairs of compounds showed significant substitution effects on viscosity sensitivity among the two different π-scaffolds included in this study.

Since molecular rotation around the single bonds of the probes is expected to occur for both the ground and excited states under ambient conditions, DFT calculations were performed for both the ground (S_0) and excited (S_1) state energies as a function of torsional angles (θ and ϕ) around the single bonds between the aromatic ring and the vinyl group or the piperidine ring, respectively (Figure 3).

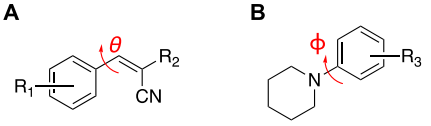

Figure 3. DFT calculations were employed to estimate the ground state and excited state energies as a function of rotation around bonds θ and ϕ. (A) The red arrow indicates the angle of rotation θ in DFT calculations, R_1 indicates the rest of the aromatic system, and R_2 indicates the water-solubilizing group. (B) The red arrow indicates the angle of rotation ϕ in DFT calculations, and R_3 indicates the rest of the compound.

The calculated relative torsional energies at different θ angles in the ground (S_0) and excited state (S_1) for the four probes are shown in Figure 4 (for an alternative plot of the data from Figure 4 that displays the S_0 and S_1 rotational energy curves aligned at a starting point of 0 kcal/mol on the same y axis, please see Figure S4). Interestingly, in the ground state, ARCAM (**1**), probe **6**, and probe **7** all exhibited minimal energies when in planar or near-planar conformations ($\theta \approx 0°$), while probe **2** preferred to be rotated out of planarity (where $\theta \approx -50°$). Probe **2** also exhibited a larger barrier to rotation (~7 kcal/mol) than **1** (~5 kcal/mol) in the ground state (from points 1 to 2), while probe **6** had a larger ground state rotational barrier (~7 kcal/mol) than **7** (~5 kcal/mol). However, the opposite trend was found when comparing the energies versus torsional angles θ of these probes in their excited states. It is important to note that for the excited state, we focused on the energetic barrier to rotate out of planarity (from points 3 to 4) since fluorescence emission is predominantly observed when the probe is in its planar state.[13,32] In this case, probe **1** had a rotational barrier (~9 kcal/mol) larger than that of **2** (~6 kcal/mol), while **7** had a much larger energetic barrier to rotation (~33 kcal/mol) than that of **6** (~1 kcal/mol). For the naphthyl probes, these calculations imply that it is easier for probe **2** to rotate and overcome the rotational energy barrier than for **1** in the excited state, which is consistent with the experimental observation that probe **2** has a higher viscosity sensitivity compared to **1** (Figure 2). Comparison of benzyl probes **6** and **7** reveals that probe **6** has a lower rotational barrier than **7** in the excited state, which is consistent with its observed larger viscosity sensitivity than **7**. These calculations suggest that it is the

https://doi.org/10.1021/acs.jpcb.4c00033
J. Phys. Chem. B 2024, 128, 3946−3952

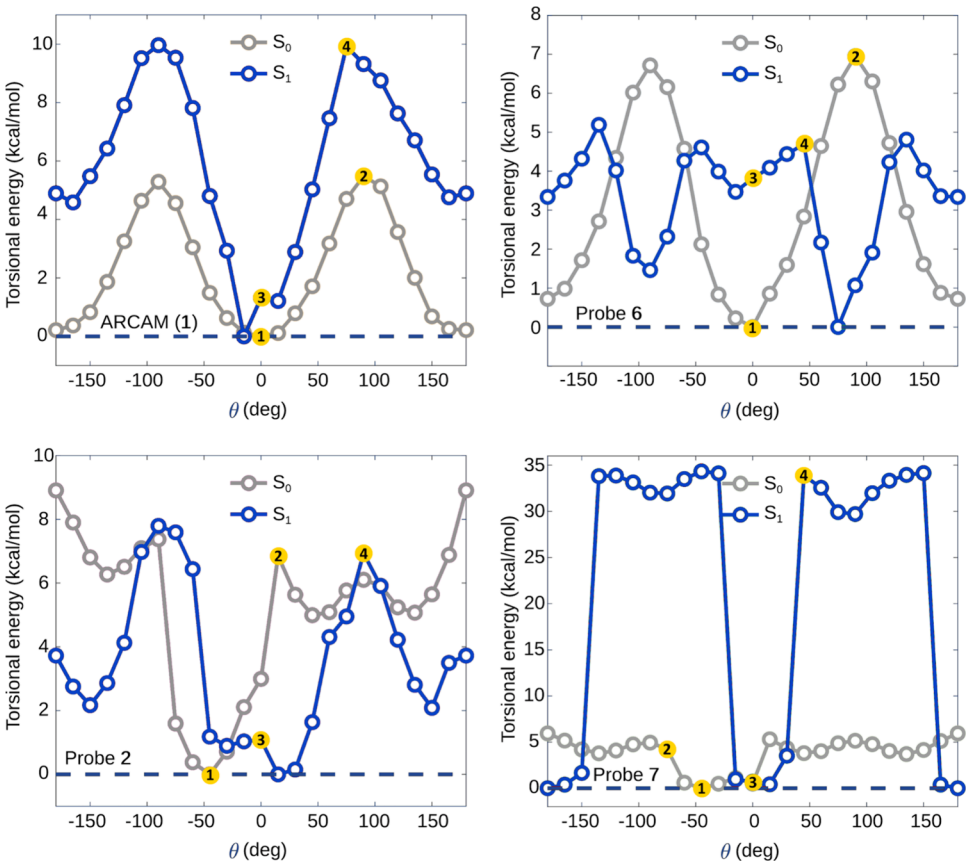

Figure 4. Torsional energy changes across the angle of the aromatic-vinyl single bond (θ) for both ground (S_0) and excited (S_1) states for probes **1**, **2**, **6**, and **7**. Ground state rotational energy barriers are calculated between points 1 and 2. Excited state rotational energy barriers are calculated between points 3 and 4.

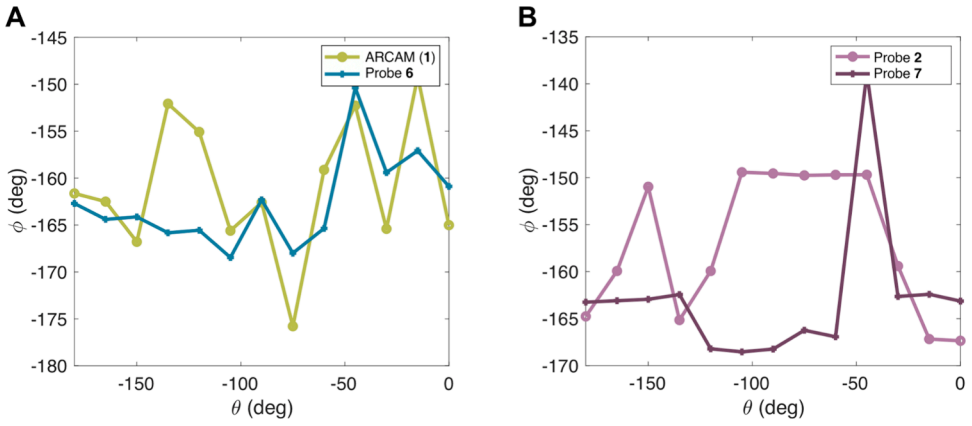

Figure 5. (A, B) Computed relationship between dihedral angles θ between the aromatic ring and the vinyl group and ϕ between the aromatic ring and the piperidine.

excited state rotational energy barrier that dominates the viscosity sensitivity of these probes.

Interestingly, probe 7 exhibited completely different behavior than the other three probes in the excited state. Specifically, the large excited state energetic barrier to rotation (~33 kcal/mol) suggests that this probe strongly prefers to stay planar while in the excited state. This property is attributed to the presence of a conical intersection[33] located between the ground state (S_0) and the first excited state (S_1). This type of conical intersection is observed when the conjugated bonds in polyenes undergo a torsional shift.[34] At the point of intersection, the potential energy surfaces of the two states converge, resulting in a notably small energy gap between the states. The large magnitude of derivative coupling between the ground and excited state in the planar structure further supports the presence of a conical intersection (Figures S5 and S6). Due to this conical intersection, probe 7 in a planar conformation exhibits a pronounced decrease in vertical excitation energy compared to probes **1**, **2**, and **6** (Figure S7). Conversely, as the twisting of the conjugated bond increases, the vertical excitation energy of probe 7 elevates. Probe **2** does not exhibit this same phenomenon due to the reduced double-

https://doi.org/10.1021/acs.jpcb.4c00033
J. Phys. Chem. B 2024, 128, 3946−3952

bond character between the aromatic ring and the vinylic carbon (as shown in Figure S5).

When performing these DFT calculations, we considered that while the only structural changes between these probes in their respective systems were the presence of the methyl group on the vinylic position, the rotation between the aryl ring and the piperidine group (Figure 3B) is also essential for fluorescence and may be affected by the vinylic substitutions (although distal from the piperidine group). The relationship between the dihedral angles of θ and ϕ is shown in Figure 5. For all four probes, when θ is at 0°, ϕ is calculated to be between −160 and −170°, so there are no major differences in the piperidinyl torsional angle between the probes. Additionally, all four probes have ϕ values that only range between −180 and −135° across all θ values, implying that the piperidine ring exhibits only minor variations in its torsional angle, rather than adopting the full range of rotational angles available. Thus, we concluded that ϕ does not appear to play a large role in affecting the relative viscosity sensitivity of these probes. This conclusion is also supported by the observation that probes **4** and **5** showed no major changes in viscosity sensitivity compared to ARCAM (**1**) (Figure 2).

CONCLUSIONS

In conclusion, the viscosity sensitivity of molecular rotor probes based on the ARCAM scaffold can be affected by small aliphatic substituents at the periphery of the π-network, in the case of probes with both a naphthyl and a benzyl π-network. In the case of the naphthyl core, introducing substituents on the vinylic position caused an enhancement in viscosity sensitivity, while substituents on the 2-piperidinyl position did not cause any significant changes. In the case of the benzyl core, introducing a substituent on the vinylic position caused the viscosity sensitivity to decrease compared with the parent probe. Computational analysis of a selection of the probes indicated that the probes exhibited a higher viscosity sensitivity when they had a lower rotational energy barrier in the excited state, which is in agreement with the solution data. This information forms the basis for a predictive model for the future probe design of viscosity sensors, which may have applications in the study of microviscosity environments associated with different diseases.

ASSOCIATED CONTENT

Supporting Information

The Supporting Information is available free of charge at https://pubs.acs.org/doi/10.1021/acs.jpcb.4c00033.

Additional details for the synthesis of probes **6** and **7**, the estimations of quantum yields, the estimation of viscosity sensitivity, and computational analysis (PDF)

AUTHOR INFORMATION

Corresponding Author

Jerry Yang − *Department of Chemistry and Biochemistry, University of California, San Diego, La Jolla, California 92093-0358, United States;* orcid.org/0000-0002-8423-7376; Email: jerryyang@ucsd.edu

Authors

Rachel S. Ehrlich − *Department of Chemistry and Biochemistry, University of California, San Diego, La Jolla, California 92093-0358, United States*

Saswata Dasgupta − *Department of Chemistry and Biochemistry, University of California, San Diego, La Jolla, California 92093-0358, United States;* orcid.org/0000-0002-8014-8376

R. Erin Jessup − *Department of Chemistry and Biochemistry, University of California, San Diego, La Jolla, California 92093-0358, United States*

Kristine L. Teppang − *Department of Chemistry and Biochemistry, University of California, San Diego, La Jolla, California 92093-0358, United States*

Alexander L. Shiao − *Department of Chemistry and Biochemistry, University of California, San Diego, La Jolla, California 92093-0358, United States*

Kun Yong Jeoung − *Department of Chemistry and Biochemistry, University of California, San Diego, La Jolla, California 92093-0358, United States*

Xuanmin Su − *Department of Chemistry and Biochemistry, University of California, San Diego, La Jolla, California 92093-0358, United States*

Aashish Shivkumar − *Department of Chemistry and Biochemistry, University of California, San Diego, La Jolla, California 92093-0358, United States*

Emmanuel A. Theodorakis − *Department of Chemistry and Biochemistry, University of California, San Diego, La Jolla, California 92093-0358, United States;* orcid.org/0000-0001-9845-6919

Francesco Paesani − *Department of Chemistry and Biochemistry, University of California, San Diego, La Jolla, California 92093-0358, United States;* orcid.org/0000-0002-4451-1203

Complete contact information is available at: https://pubs.acs.org/10.1021/acs.jpcb.4c00033

Author Contributions

R.S.E. and J.Y. conceived and designed the research. R.S.E., S.D., F.P., E.A.T., and J.Y. analyzed the data. R.S.E., S.D., R.E.J., K.L.T., A.L.S., K.Y.J., X.S., and A.S. executed the experiments. R.S.E. and J.Y. wrote the manuscript. All authors reviewed and edited the manuscript.

Funding

This work was supported by the National Institute on Aging of the National Institutes of Health under award nos. 1RF1AG062362 and 1RF1AG077802 and National Science Foundation through award no. 2311260 (F.P.). This research used Expanse at the San Diego Supercomputer Center (SDSC) through allocation CHE230052 from the Advanced Cyberinfrastructure Coordination Ecosystem: Services & Support (ACCESS) program, which is supported by National Science Foundation grant nos. 2138259, 2138286, 2138307, 2137603, and 2138296. The content is solely the responsibility of the authors and does not necessarily represent the official views of the National Institutes of Health or the National Science Foundation.

Notes

The authors declare the following competing financial interest(s): J.Y. is a founder and equity interest holder of Amydis, Inc. All other authors declare no competing financial or non-financial interests.

■ ACKNOWLEDGMENTS

We would like to thank Professors Yitzhak Tor and Judy Kim for their helpful guidance during the execution of these experiments.

■ REFERENCES

(1) Haidekker, M. A.; Brady, T. P.; Lichlyter, D.; Theodorakis, E. A. Effects of Solvent Polarity and Solvent Viscosity on the Fluorescent Properties of Molecular Rotors and Related Probes. *Bioorg. Chem.* **2005**, *33* (6), 415−425.

(2) Lee, S. C.; Heo, J.; Woo, H. C.; Lee, J. A.; Seo, Y. H.; Lee, C. L.; Kim, S.; Kwon, O. P. Fluorescent Molecular Rotors for Viscosity Sensors. *Chem. − Eur. J.* **2018**, *24* (52), 13706−13718.

(3) Vázquez, B. Y. S.; Cabrales, P.; Tsai, A. G.; Johnson, P. C.; Intaglietta, M. Lowering of Blood Pressure by Increasing Hematocrit with Non−Nitric Oxide−Scavenging Red Blood Cells. *Am. J. Cell Mol. Biol.* **2008**, *38* (1), 135−142.

(4) Luneva, O. G.; Brazhe, N. A.; Maksimova, N. V.; Rodnenkov, O. V.; Parshina, E. Y.; Bryzgalova, N. Y.; Maksimov, G. V.; Rubin, A. B.; Orlov, S. N.; Chazov, E. I. Ion Transport, Membrane Fluidity and Haemoglobin Conformation in Erythrocyte from Patients with Cardiovascular Diseases: Role of Augmented Plasma Cholesterol. *Pathophysiology* **2007**, *14* (1), 41−46.

(5) Aleardi, A. M.; Benard, G.; Augereau, O.; Malgat, M.; Talbot, J. C.; Mazat, J. P.; Letellier, T.; Dachary-Prigent, J.; Solaini, G. C.; Rossignol, R. Gradual Alteration of Mitochondrial Structure and Function by β-Amyloids: Importance of Membrane Viscosity Changes, Energy Deprivation, Reactive Oxygen Species Production, and Cytochrome c Release. *J. Bioenerg. Biomembr.* **2005**, *37* (4), 207−225.

(6) Miao, W.; Yu, C.; Hao, E.; Jiao, L. Functionalized BODIPYs as Fluorescent Molecular Rotors for Viscosity Detection. *Front. Chem.* **2019**, *7*, 825.

(7) Hou, M. X.; Liu, L. Y.; Wang, K. N.; Chao, X. J.; Liu, R. X.; Mao, Z. W. A Molecular Rotor Sensor for Detecting Mitochondrial Viscosity in Apoptotic Cells by Two-Photon Fluorescence Lifetime Imaging. *New J. Chem.* **2020**, *44* (26), 11342−11348.

(8) Stsiapura, V. I.; Maskevich, A. A.; Kuzmitsky, V. A.; Uversky, V. N.; Kuznetsova, I. M.; Turoverov, K. K. Thioflavin T as a Molecular Rotor: Fluorescent Properties of Thioflavin T in Solvents with Different Viscosity. *J. Phys. Chem. B* **2008**, *112* (49), 15893−15902.

(9) Sutharsan, J.; Dakanali, M.; Capule, C. C.; Haidekker, M. A.; Yang, J.; Theodorakis, E. A. Rational Design of Amyloid Binding Agents Based on the Molecular Rotor Motif. *ChemMedChem.* **2010**, *5* (1), 56−60.

(10) Sutharsan, J.; Lichlyter, D.; Wright, N. E.; Dakanali, M.; Haidekker, M. A.; Theodorakis, E. A. Molecular Rotors: Synthesis and Evaluation as Viscosity Sensors. *Tetrahedron* **2010**, *66* (14), 2582−2588.

(11) Oster, G.; Nishijima, Y. Fluorescence and Internal Rotation: Their Dependence on Viscosity of the Medium. *J. Am. Chem. Soc.* **1956**, *78* (8), 1581−1584.

(12) Loutfy, R. O.; Arnold, B. A. Effect of Viscosity and Temperature on Torsional Relaxation of Molecular Rotors. *J. Phys. Chem.* **1982**, *86* (21), 4205−4211.

(13) Ye, S.; Zhang, H.; Fei, J.; Wolstenholme, C. H.; Zhang, X. A General Strategy to Control Viscosity Sensitivity of Molecular Rotor-Based Fluorophores. *Angew. Chem.* **2021**, *133* (3), 1359−1366.

(14) Haidekker, M. A.; Theodorakis, E. A. Environment-Sensitive Behavior of Fluorescent Molecular Rotors. *J. Biol. Eng.* **2010**, 11.

(15) Haidekker, M. A.; Theodorakis, E. A. Molecular Rotors—Fluorescent Biosensors for Viscosity and Flow. *Org. Biomol. Chem.* **2007**, *5* (11), 1669−1678.

(16) Liu, X.; Chi, W.; Qiao, Q.; Kokate, S. V.; Cabrera, E. P.; Xu, Z.; Liu, X.; Chang, Y. T. Molecular Mechanism of Viscosity Sensitivity in BODIPY Rotors and Application to Motion-Based Fluorescent Sensors. *ACS Sensors* **2020**, *5* (3), 731−739.

(17) Guan, Y.; Cao, K. J.; Cantlon, A.; Elbel, K.; Theodorakis, E. A.; Walsh, D. M.; Yang, J.; Shah, J. V. Real-Time Monitoring of Alzheimer's-Related Amyloid Aggregation via Probe Enhancement-Fluorescence Correlation Spectroscopy. *ACS Chem. Neurosci.* **2015**, *6* (9), 1503−1508.

(18) Do, J. P.; Cao, K. J.; Wei, S.; Laurent, L. C.; Parast, M. M.; Yang, J. Identification of Patients with Preeclampsia by Measuring Fluorescence of an Amyloid-Binding Aryl Cyano Amide in Human Urine Samples. *Anal. Chem.* **2018**, *90* (24), 14316−14320.

(19) Cao, K. J.; Kim, J. H.; Kroeger, H.; Gaffney, P. M.; Lin, J. H.; Sigurdson, C. J.; Yang, J. ARCAM-1 Facilitates Fluorescence Detection of Amyloid-Containing Deposits in the Retina. *Transl. Vis. Sci. Technol.* **2021**, *10* (7), 5.

(20) Ehrlich, R. S.; Shiao, A. L.; Li, M.; Teppang, K. L.; Jeoung, K. Y.; Theodorakis, E. A.; Yang, J. Exploring the Effect of Aliphatic Substituents on Aryl Cyano Amides on Enhancement of Fluorescence upon Binding to Amyloid-β Aggregates. *ACS Chem. Neurosci.* **2021**, *12* (15), 2946−2952.

(21) Jones, G.; Jackson, W. R.; Choi, C. Y.; Bergmark, W. R. Solvent Effects on Emission Yield and Lifetime for Coumarin Laser Dyes. Requirements for a Rotatory Decay Mechanism. *J. Phys. Chem.* **1985**, *89* (2), 294−300.

(22) Eaton, D. F. Reference Materials for Fluorescence Measurement. *Pure Appl. Chem.* **1988**, *60* (7), 1107−1114.

(23) Lebel, R. G.; Goring, D. A. I. Density, Viscosity, Refractive Index, and Hygroscopicity of Mixtures of Water and Dimethyl Sulfoxide. *J. Chem. Eng. Data* **1962**, *7* (1), 100−101.

(24) Moutzouris, K.; Papamichael, M.; Betsis, S. C.; Stavrakas, I.; Hloupis, G.; Triantis, D. Refractive, Dispersive and Thermo-Optic Properties of Twelve Organic Solvents in the Visible and near-Infrared. *Appl. Phys. B Lasers Opt.* **2014**, *116* (3), 617−622.

(25) Ghobashy, M. M. Greener Synthesis of Carbon Dots. *Handb. Greener Synth. Nanomater. Compd.* **2021**, 219−244.

(26) Sinkeldam, R. W.; Wheat, A. J.; Boyaci, H.; Tor, Y. Emissive Nucleosides as Molecular Rotors. *ChemPhysChem* **2011**, *12* (3), 567−570.

(27) Epifanovsky, E.; Gilbert, A. T. B.; Feng, X.; Lee, J.; Mao, Y.; Mardirossian, N.; Pokhilko, P.; White, A. F.; Coons, M. P.; Dempwolff, A. L.; et al. Software for the Frontiers of Quantum Chemistry: An Overview of Developments in the Q-Chem 5 Package. *J. Chem. Phys.* **2021**, *155* (8), No. 084801, DOI: 10.1063/5.0055522. (For the full citation including the list of all authors, please see the Supporting Information).

(28) Chai, J. Da; Head-Gordon, M. Long-Range Corrected Hybrid Density Functionals with Damped Atom−Atom Dispersion Corrections. *Phys. Chem. Chem. Phys.* **2008**, *10* (44), 6615−6620.

(29) Dasgupta, S.; Herbert, J. M. Standard Grids for High-Precision Integration of Modern Density Functionals: SG-2 and SG-3. *J. Comput. Chem.* **2017**, *38* (12), 869−882.

(30) Förster, T.; Hoffmann, G. Die Viskositätsabhängigkeit Der Fluoreszenzquantenausbeuten Einiger Farbstoffsysteme. *Z. Phys. Chem.* **1971**, *75*, 63−76.

(31) Diamandis, E. P.; Christopoulos, T. K. Fluorescence Immunoassays. In *Immunoassay*; Academic Press, 1996; pp 309−335.

(32) Freire, S.; De Araujo, M. H.; Al-Soufi, W.; Novo, M. Photophysical Study of Thioflavin T as Fluorescence Marker of Amyloid Fibrils. *Dye. Pigment.* **2014**, *110*, 97−105.

(33) Bernardi, F.; Olivucci, M.; Robb, M. A. Potential Energy Surface Crossings in Organic Photochemistry. *Chem. Soc. Rev.* **1996**, *25* (5), 321−328.

(34) Ben-Nun, M.; Martínez, T. J. Photodynamics of Ethylene: Ab Initio Studies of Conical Intersections. *Chem. Phys.* **2000**, *259* (2−3), 237−248.